Available online at www.sciencedirect.com

jmr&t Journal of Materials Research and Technology

https://www.journals.elsevier.com/journal-of-materials-research-and-technology

Original Article

Effects of environmental actions, recycled aggregate quality and modification treatments on durability performance of recycled concrete

Bin Lei[a,b], *Wengui Li*[b,*], *Zhuo Tang*[b], *Zhaohang Li*[a], *Vivian W.Y. Tam*[c]

[a] *School of Civil Engineering and Architecture, Nanchang University, Jiangxi 330031, China*
[b] *School of Civil and Environmental Engineering, University of Technology Sydney, NSW 2007, Australia*
[c] *School of Built Environment, Western Sydney University, NSW 2751, Australia*

ARTICLE INFO

Article history:
Received 5 May 2020
Accepted 15 September 2020
Available online 30 September 2020

Keywords:
Recycled aggregate
Recycled concrete
Modification treatment
Environmental action
Durability

ABSTRACT

The durability performance of recycled concrete (RC) subjected to different environmental actions, including salt-solution, mechanical load, salt-solution freeze-thaw cycles, and coupled mechanical load and salt-solution freeze-thaw cycles was investigated in this paper. To evaluate the effects of recycled aggregate (RA) quality on the RC durability, modeled recycled concrete (MRC) containing modeled recycled aggregate (MRA) with various thickness and coverage of old mortar, along with different degrees of initial damage, was fabricated and tested. Moreover, several modification treatments were employed to study the effects of modification treatments on the RC durability, which included the impregnation of RA with polyvinyl alcohol (PVA) emulsion or nano-SiO_2 solutions, and the enhancement of RC with the incorporations of fly ash or hybrid fly ash and silica fume. The results reveal that the deterioration of RC under coupled actions of mechanical load and salt-solution freeze-thaw cycles was the most severe, which was followed by the salt-solution freeze-thaw cycles, mechanical load and salt-solution. The old interface in RA was determined as the weakest zone in RC. With the increase in the thickness or coverage of old mortar, or the initial damage of RA, the durability performance of RC declined, and the effect of initial damage of RA was more significant compared to the thickness or coverage of old mortar. Additionally, modifying RC with 1.5% nano-SiO_2 solution or PVA emulsion, and replacing cement with 10% fly ash can significantly enhance the RC durability.

1. Introduction

According to the statistics, approximately 2 million tons of waste concrete is generated annually in China [1]. Recycling waste concrete into new concrete, that is, recycled concrete (RC), has become an effective method for concrete waste disposal [2,3]. Currently, the mechanical properties of RC materials and components have been extensively studied [4–6]. Durability, as an important requisite for the good per-

* *Corresponding author at*: School of Civil and Environmental Engineering, University of Technology Sydney, NSW 2007, Australia
E-mail: wengui.li@uts.edu.au (W. Li).

https://doi.org/10.1016/j.jmrt.2020.09.073

formance of RC, has also attracted considerable attention. In previous studies, the resistance of RC to single environmental factors, such as carbonation [7–9], chloride penetration [10–12], sulfate erosion [13–15], and freeze-thaw cycles [16–20], has been widely investigated. Also, a few studies have been carried out on the resistance of RC to combined multiple environmental factors, such as chloride penetration and loading [21–23], freeze-thaw and loading [24–26], as well as, chloride penetration, freeze-thaw, and loading [27,28]. Most of the results show that the durability of RC is generally lower than that of normal concrete (NC), and decreases with the increase of recycled aggregate (RA) replacement ratio. The results also indicated that combined multiple environmental factors would increase the deterioration rate compared to that under any single factors. Moreover, the effect of a single factor would be promoted by other factors [28].

The old mortar attached to RA is the most significant difference between RC and NC, and it is generally recognized as the main cause for the poorer properties of RC compared with NC [29–31]. The old mortar forms a new interface with the new mortars, resulting in more interfaces in RC than in NC with the same mix design. The interface, as the weakest area in concrete, causes the RC to crack easily and subsequently reduces its durability [32]. In addition, the initial damage in the RA, such as the accumulation of internal damage during the crushing process, also influences the properties of RC [33]. However, a few studies have pointed out that the unhydrated part of the cement in the old mortar can continue to hydrate and play a positive role in the internal curing [34,35]. In particular, the hydration products can not only enhance the bonding strength between the aggregate and old mortar, but also cover and fill the microcracks [36–38], therefore improving the RC properties. To investigate the effect of the old mortar on the RC, modeled recycled aggregate (MRA) and modeled recycled concrete (MRC) had been developed to simplify the real RC for the experimental study [39–41]. For instance, Xiao et al. [41] performed an experimental and analytical study to investigate the stress-strain behaviors of MRC under uniaxial compression. However, some aspects, especially the coverage thickness of the adhered old mortar and the initial damage of MRA during the service process of the original concrete and the crushing process associated with waste concrete recycling, were not considered in the previous studies [39–41]. Furthermore, the previous studies mainly focused on the mechanical properties of MRC, while limited studies on the durability of MRC under the complex or harsh environment have been reported.

To improve the strength and durability of RC, various modification methods have been explored [42]. These methods can be divided into two categories: strengthening RC integrally with the addition of admixtures and enhancing RA with modification treatments. It was reported that the addition of fly ash can increase the resistance of RA to sulfate attack and freeze-thaw cycles [43]. Mukharjee and Barai [44] found that the compressive strength of RC with 3% nano-SiO_2 was close to that of NC. The treatment of RA with nanomaterial solutions or polymer emulsion has been investigated for the enhancement of RA [45]. When RA is immersed in nanomaterial solution, the nanomaterial, such as nano-SiO_2 and nano-$CaCO_3$, can fill the pores and voids inside the adhered mortars. Besides, some nanomaterials can react with calcium hydroxide ($Ca(OH)_2$) to form C-S-H gels, which could further enhance the strength and durability properties of RC [46]. Polymers are water repellent and can be used to reduce the water absorption of porous materials. When RA was immersed in a polymer emulsion, the polymer molecules filled the pores of the adhered mortar and sealed the surfaces of RA [42]. Kou and Poon [47] concluded that the physical and mechanical properties of RA could be improved by the treatment with polyvinyl alcohol (PVA) emulsion, while only slightly better results were obtained when the concentration of PVA emulsion exceeded 10%. Moreover, PVA impregnation could increase the bonding strength between the RA and cement matrix [48]. Despite these above benefits achieved by the modification treatments, the studies on the effect of modification treatments on the durability of RC under coupled actions are very limited [42,45].

Table 1 – Physical properties of recycled aggregate.

Apparent density (kg/m^3)	Water absorption (%)	Crushing index (%)	Size distribution (mm)
2531	4.0	17.6	5–31.5

In this study, a series of experiments are conducted to investigate the effects of various environmental actions, RA quality and modification treatments on the durability of RC. The environmental actions include salt-solution, salt-solution freeze-thaw cycles, mechanical load, and coupled actions of mechanical load and salt-solution freeze-thaw cycles. Also, MRC containing MRA with different degrees of initial aggregate damage, old mortar thickness, and old mortar coverage was manufactured and tested, to understand the effect of old mortar attached to RA on the durability of RC. Moreover, the durability of RC after the treatment of RA with nano-SiO_2 solution or PVA emulsion, or the inclusion of fly ash or the admixture of fly ash and silica fume, was also investigated. Further, the microstructure of the interfacial transition zones (ITZs) in MRC was characterized by scanning electron microscopy (SEM).

2. Experimental program

2.1. *Raw materials*

The RA used for fabricating RC specimens was prepared in the laboratory by crushing the demolished concrete waste from an old building, as shown in Fig. 1. The physical properties of the RA are given in Table 1. The sand used was based on the river sand sourced from Ganjiang River, China, which had a fineness modulus of 2.45 and an apparent density of 2688 kg/m^3. Ordinary Portland cement (Grade 42.5) supplied by Huaihai Co., Ltd., China, was used as the cementitious binder. The chemical compositions of the cement are presented in Table 2. Tap water was used for concrete mixing. The salt solution with a concentration of 10% was prepared by mixing sodium sulfate, sodium chloride, and magnesium chloride with a ratio of 1.0:1.0:1.0. Fly ash and silica fume were used as the admixtures for the RC modification, and their chemical compositions are listed in Table 2. PVA powder was used for enhancing RA, whose chemical compositions are provided in Table 3. Besides,

Fig. 1 – Resource and manufacturing of recycled aggregates.

Table 2 – Chemical composition of cementitious materials.

	SiO_2	Al_2O_3	CaO	MgO	Fe_2O_3	SO_3	K_2O	Na_2O	Total
Portland cement	21.92	7.63	60.1	2.59	2.60	2.53	0.26	0.32	97.99
Fly ash	56.10	26.24	5.57	1.20	5.34	1.21	1.93	0.28	97.87
Silica fume	93.42	0.33	1.71	0.30	0.82	——	0.76	0.23	97.57

Table 3 – Chemical composition of polyvinyl alcohol (PVA) powder (%).

PVA	Volatile	Sodium acetate	Ash
91.7	5.0	2.8	0.5

commercial nano-SiO_2 solution with a concentration of 30% was used for the RA modification treatment, and its properties are presented in Table 4.

2.2. *Specimen preparation*

2.2.1. *Recycled concrete*

The water to cement ratio was 0.49. The amounts of cement, sand, water, and RA in RC per cubic meter were 398, 546, 195, and 1161 kg, respectively. The fresh concrete was cast into 100 × 100 × 100 mm cubic moulds according to the code of GB/T50081-2002 [49].

2.2.2. *Modeled recycled aggregate*

The mix proportion of mortar in MRC was the same as that in RC, which was 1: 2.04: 2.8 for water: cement: sand. The manufacturing process of MRA is shown in Fig. 2(a). Specifically, granite plates were cut into the prism with a dimension of 15 × 15 × 50 mm by a cutting machine, and then cement mortar with a thickness of 2, 4, or 6 mm was cast on the surface, as shown in Fig. 2(b). Then, the MRAs were cured under a temperature of 20 ± 2 °C and relative humidity of 95% for 28 days. Additionally, to simulate the different coverage of old mortar in RA, the MRA with 4 mm thickness of the old cement was cut into different coverage percentages, including 50%, 75%, and 100%, as shown in Fig. 2(c). Moreover, in order to simulate the initial damage caused during the service process of the original concrete and the crushing process of RA, the MRA was subjected to different salt-solution freeze-thaw cycles. Fig. 3 presents the MRAs obtained after the exposure to different salt-solution freeze-thaw cycles. Obviously, the MRAs experienced the loss of attached mortar at edges and corners after the freeze-thaw cycles. Also, the damage was more serious, with the increase in the freeze-thaw cycles.

Table 5 – Different types of modeled recycled concrete prepared.

Specimen	Old mortar thickness (mm)	Old mortar coverage (%)	Initial freeze-thaw cycles
MRC-D0-T4	4	100%	0
MRC-D10-T4	4	100%	10
MRC-D20-T4	4	100%	20
MRC-D30-T4	4	100%	30
MRC-D40-T4	4	100%	40
MRC-D50-T4	4	100%	50
MRC-C100-T2	2	100%	50
MRC-C100-T4	4	100%	50
MRC-C100-T6	6	100%	50
MRC-C50-T4	4	50%	50
MRC-C75-T4	4	75%	50

2.2.3. *Modeled recycled concrete*

Total 9 MRAs and new mortar (with the proportion of water: cement: sand = 1: 2.04: 2.8) were cast into the MRC specimen with a dimension of 100 × 100 × 50 mm. After 24 h curing, the specimen was demolded and placed in a standard curing chamber (at temperature of 20 ± 2 °C and 95% relative humidity) for 28 days. The details of the prepared MRC are summarized in Table 5. In Table 5, the specimens were labeled as follows. D0, D10, D20, D30, D40, and D50 denote the number of freeze-thaw cycles for MRAs (i.e., 0, 10, 20, 30, 40, and 50 cycles, respectively); C50%, C75%, and C100% represent the coverage percentage of old mortar in MRAs (i.e., 50%, 75%, and

Table 4 – Properties of nano-SiO_2 solution.

Concentration of SiO_2	Concentration of Na_2O	PH value	Density	Particle size
30 ± 1%	≤0.2%	6.5–8.0	1.19–1.21 g/cm^3	8–15 nm

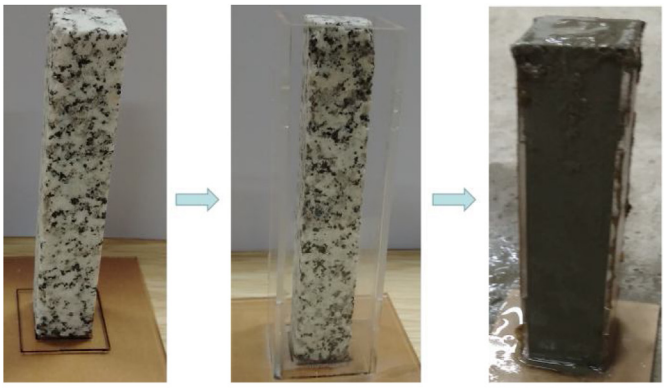

(a) Manufacturing process of MRAs

(b) Different degrees of old mortar thickness (c) Different degrees of coverage of old mortar

Fig. 2 – MRA prepared with different thickness and coverage of old mortar.

(a) 10 cycles (b) 30 cycles (c) 50 cycles

Fig. 3 – MRA subjected to different salt-solution freeze-thaw cycles.

100%, respectively); T2, T4, and T6 indicate the thickness of the old mortar in MRAs (i.e., 2, 4, and 6 mm, respectively). The prepared MRC is shown in Fig. 4.

2.2.4. *Modification treatment for RC*

In this study, several methods were considered for the modification of RC, including the impregnation of RA with PVA emulsion or nano-SiO_2 solution, and the enhancement of RC with the inclusion of fly ash or the admixture of fly ash and silica fume. The mixture proportion of the modified RC was the same as that in RC, which was 398, 546, 195, and 1161 kg/m^3 for cement, sand, water, and RA, respectively. All the specimens were cast into 100 × 100 × 100 mm cubes, according to the GB/T50081-2002 [49].

The concentrations of the PVA emulsion and nano-SiO_2 solution adopted in this study included 0.5%, 1.0%, and 1.5%. First, the PVA emulsion or nano-SiO_2 solution with the target concentration was prepared. For the preparation of PVA immersion, the PVA powder was slowly added into tap water at 20 °C while slowly stirring to prevent the powder from caking. The stirring speed was 70–100 r/min. Next, the RA was added into the bucket and was immersed for 120 min. Subsequently, the RA was removed from the bucket, and a screen was used to remove the redundant PVA emulsion or nano-SiO_2 solution adhering to the RA. Finally, the RA was dried at 20 ± 2 °C and 64 ± 5% relative humidity for 3 days. Fig. 5 displays the impregnation treatment of RA using PVA emulsion.

For the group with the incorporation of fly ash, the replacement percentages of cement by fly ash included 10%, 20%, and 30%, which were labeled as RCF10, RCF20, and RCF30, respectively. For the group incorporated with hybrid fly ash

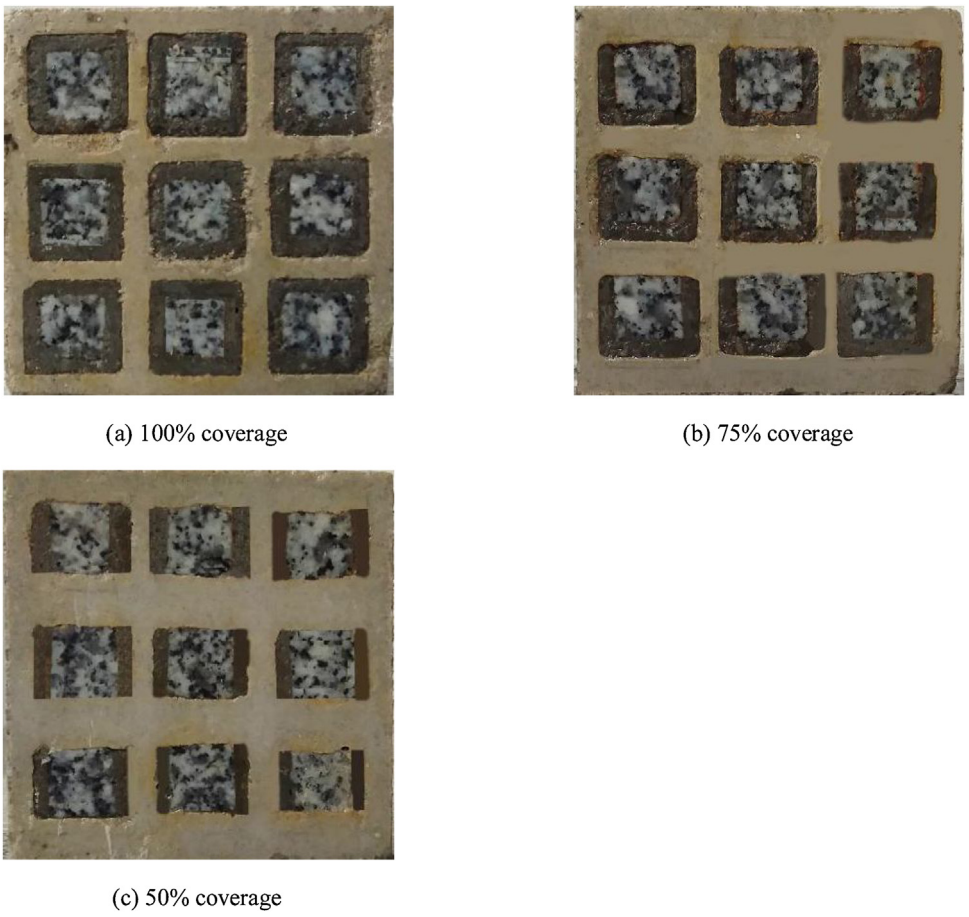

Fig. 4 – Modeled recycled concrete specimen prepared for durability test.

Fig. 5 – Modification treatment of recycled aggregate using PVA emulsion.

and silica fume, the replacement percentage of cement with the admixture of fly ash and silica fume was 20%, and different proportions of fly ash and silica fume were employed. Specifically, 15% fly ash and 5% silica fume, 10% fly ash and 10% silica fume, as well as, 5% fly ash and 15% silica fume, were considered and labeled as RCF15S5, RCF10S10, and RCF5S15, respectively.

2.3. *Durability investigation*

The RC, MRC, and modified RC specimens prepared were employed in different durability tests. Specifically, RC specimens were subjected to various environmental actions to study the effect of environmental factors, while MRC and modified RC specimens were subjected to the coupled actions of mechanical load and salt-solution freeze-thaw cycles to study the effects of the RA quality and modification treatment, respectively. Fig. 6 illustrates the details of these experiments.

The RC specimens were divided into five groups, which are listed in Table 6. Each group had three nominally identical specimens. The specimens in the control group (RC-C0-L0) and salt-solution group (RC-C10-L0) were immersed in water and salt-solution, respectively. The specimens in the group

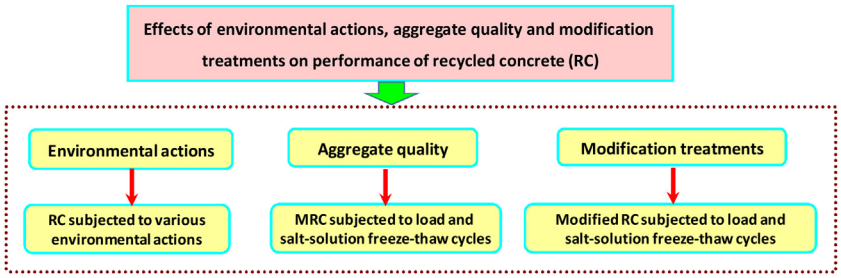

Fig. 6 – Schematic diagram of the process of experimental program.

Table 6 – Compressive strengths of recycled concrete under various environmental actions.

Various actions	Specimen	Immersion solution	Stress level	Freeze-thaw cycles	Alternative times of load	Compressive strength (MPa)	
						Mean	Deviation
Control	RC-C0-L0	Water	0	0	0	53.20	1.28
Salt-solution	RC-C10-L0	10% salt- solution	0	0	0	51.71	6.00
Mechanical load	RC-C0-L30	Water	30%	0	5	49.79	4.08
	RC-C0-L50	Water	50%	0	5	46.41	5.38
Salt-solution freeze-thaw cycle	RC-F10-L0	10% salt- solution	0	50	0	44.95	5.86
Coupled actions of load and	RC-F10-L50-1	10% salt- solution	50%	50	1	44.00	7.51
salt-solution freeze-thaw cycle	RC-F10-L50-2	10% salt- solution	50%	50	2	42.67	8.56
	RC-F10-L50-5	10% salt- solution	50%	50	5	38.56	0

Notes: C0 and C10 represent the concentrations of the corrosion solution given as 0% and 10%, respectively; L0, L30, and L50 represent the stress levels given as 0%, 30%, and 50%, respectively; F10 represents the freeze-thaw cycle in salt-solution with a concentration of 10%. For the group under the coupled actions of load and salt-solution freeze-thaw cycles, 1, 2, and 5 represent the alternative times of repetitive loading.

under salt-solution freeze-thaw (RC-F10-L0) were subjected to 50 freeze-thaw cycles in salt-solution. For the group under the coupled actions of mechanical load and salt-solution freeze-thaw cycles (RC-F10-L50-1, RC-F10-L50-2, and RC-F10-L50-5), the test protocols are presented in Fig. 7(a–c) [28]. Specifically, the specimens were loaded and unloaded for five times at the stress level of 50% (the ratio of the applied stress to 28 d compressive strength). Afterward, the specimens were put into the freeze-thaw machine for 50, 25, or 10 cycles in salt-solution. The procedures were repeated until 50 freeze-thaw cycles were completed. In the group under mechanical load (RC-C0-L30, RC-C0-L50), the specimens were loaded for 5 times at 30% or 50% stress level, which was followed by immersion in water. The test for the group under mechanical load was carried out simultaneously with the test for the group under the coupled actions of loading and salt-solution freeze-thaw cycles. While the specimens (RC-F10-L50-5) for coupled actions were subjected to freeze-thaw cycles after loading, the specimens (RC-C0-L30, RC-C0-L50) for mechanical load test were immersed water, as shown in Fig. 7(d). After these processes, the compressive strengths of all the specimens in five groups were measured.

For one salt-solution freeze-thaw cycle, the specimens were first frozen at a constant temperature of −20 °C for 6 h, and subsequently, the specimens were transferred to the prepared salt solution at a temperature of 20 °C for 4 h, as per GB/T50082-2009 [50]. The repeated loading operation was as follows. First, the specimen was preloaded to 15% stress level of the ultimate strength to ensure that the system worked properly and the specimen was tightly clamped in the test machine. Second, the load was applied to the specimen to the targeted stress level and maintained for 30 s, which was followed by unloading to a stress-free state. The loading and unloading rates were set as 0.5 MPa/s, according to GB/T50081-2002 [49].

As for the test on the effects of the RA quality and modification treatment on the durability of RC, the durability tests were performed on the MRC and modified RC specimens, respectively, by employing the durability test protocol in Fig. 7(b). Specifically, the MRC and modified RC specimens were subjected to 2 times of the repeated loading at a stress level of 50% and the following 25 salt-solution freeze-thaw cycles. The compressive strengths of the specimens before and after the above process were measured, and the result presented was the average of three duplicated specimens.

2.4. *Microstructure characterization*

To further understand the deterioration mechanism under the coupled actions of mechanical load and salt-solution freeze-thaw cycles, the microstructure of ITZs in MRC, before and after the coupled actions, were characterized by scanning electron microscopy (SEM). Core parts of the MRC specimen before and after the coupled actions were taken, which had a cross section of 10 × 10 mm and a thickness of 5 mm. After coating with carbon, the samples were observed by SEM. Three points were randomly selected within the old and new ITZs.

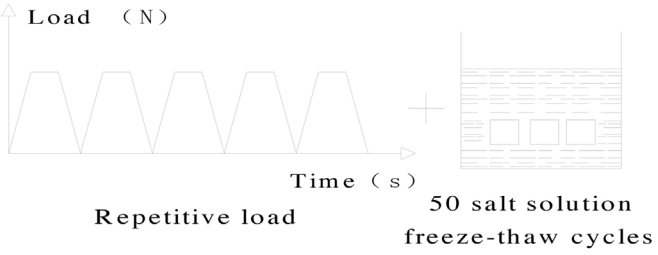

(a) One alternative time of repetitive loading and freeze-thaw cycles (RC-F10-L50-1)

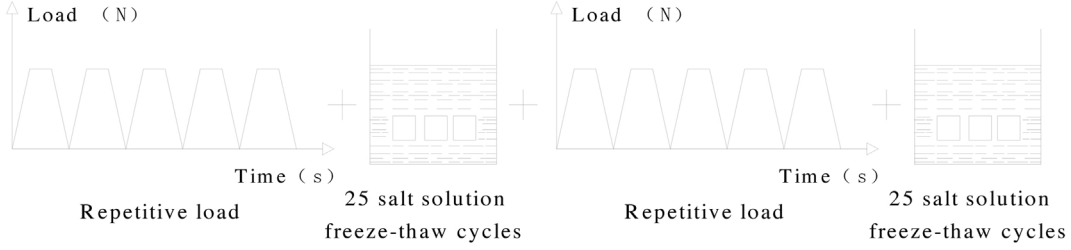

(b) Two alternative times of repetitive loading and freeze-thaw cycles (RC-F10-L50-2)

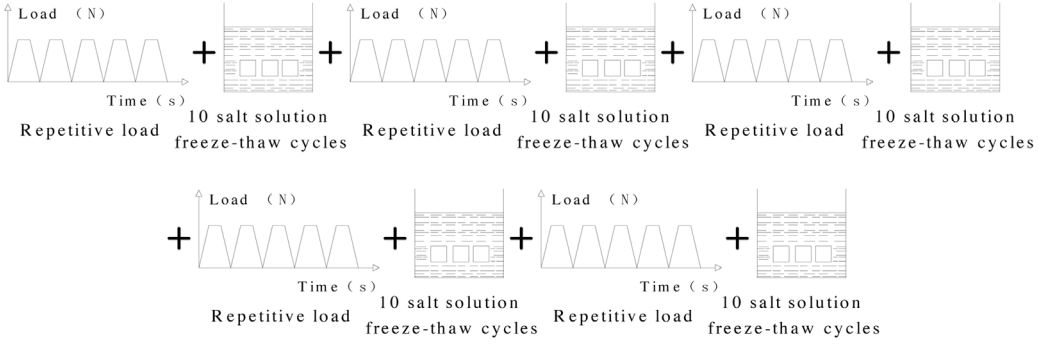

(c) Five alternative times of repetitive loading and freeze-thaw cycles (RC-F10-L50-5)

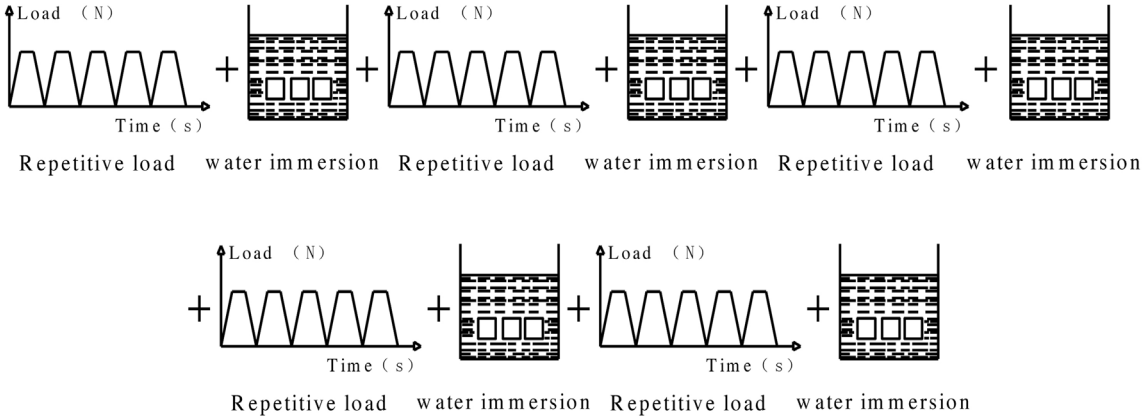

(d) Five alternative times of repetitive loading and water immersion (RC-C0-L30 and RC-C0-L50)

Fig. 7 – Schematic diagram for the durability test protocols for recycled concrete (Lei et al., 2018).

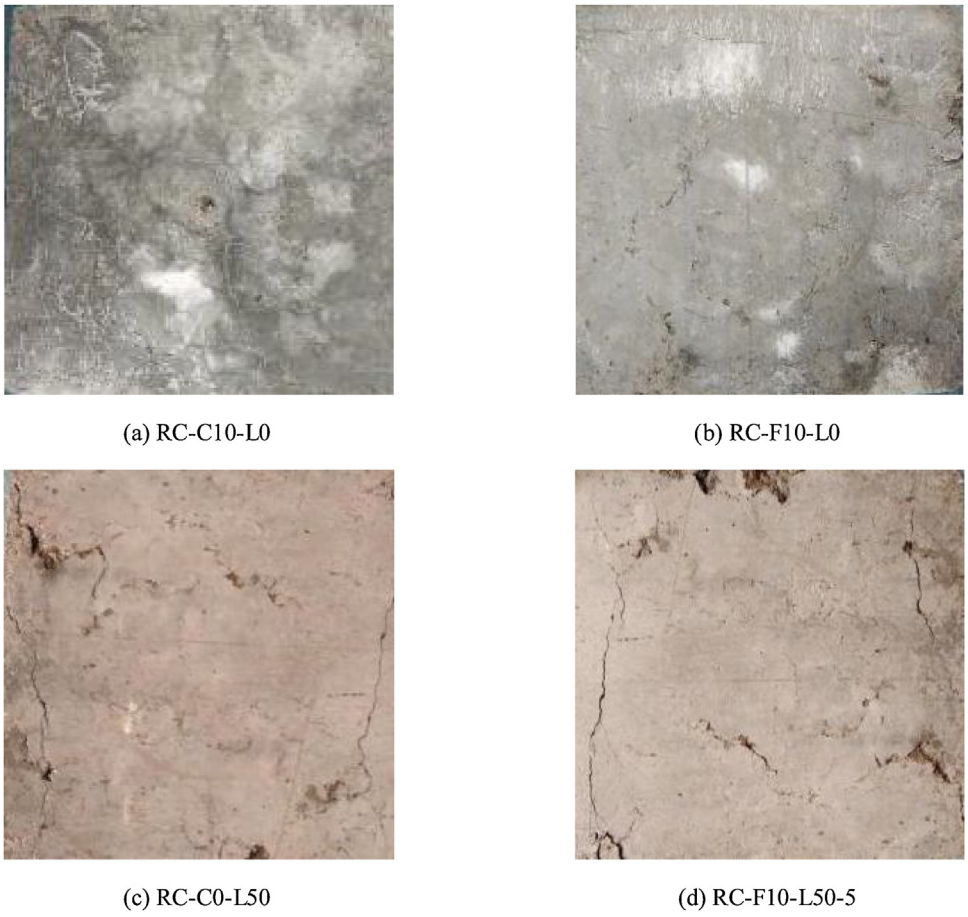

(a) RC-C10-L0 (b) RC-F10-L0

(c) RC-C0-L50 (d) RC-F10-L50-5

Fig. 8 – Damage patterns of RC subjected to various environmental actions.

3. Results and discussions

3.1. *Effects of environmental actions*

3.1.1. *Failure pattern*

The typical patterns of the specimens after different environmental actions are shown in Fig. 8. For the group subjected to salt-solution (RC-C10-L0), the specimen exhibited an intact surface without spalling at the edges or corners in Fig. 8(a). For the group subjected to salt-solution freeze-thaw cycles (RC-C10-L0), and the group subjected to mechanical loading (RC-C0-L50), only a few vertical cracks and small peeling pieces at the edge were observed in Fig. 8(b) and (c). However, the failure of group RC-F10-L50-5, which was subjected to the coupled actions of mechanical load and salt-solution freeze-thaw cycles, was quite significant. As shown in Fig. 8(d), many cracks and spalling on the surface of the specimen could be seen. Besides, white salt crystals attached to the surface of the specimen could be identified.

The coupled actions exerted both physical and chemical effects on the deterioration of the RC. At the early stage, several microcracks were produced, attributed to the mechanical loading. After that, the concrete interior generated more microcracks due to the swelling stress by the freeze-thaw cycles, which further increased the permeability of the concrete. Meanwhile, SO_4^{2-} and Mg^{2+} in the salt-solution could more easily penetrate into the concrete and react with $Ca(OH)_2$. The reaction products such as ettringite and gypsum could accumulate in the cracks and increase the swelling stress in the concrete. The cohesionless reaction products of $Mg(OH)_2$ also facilitated the further deterioration of the concrete. Moreover, the subsequent cyclic loading continued to accelerate the propagation of cracks further [51]. As a result, the combined effect of physical and chemical corrosion under the coupled actions facilitated the expansion and connection of the cracks, resulting in severe performance deterioration in the RC.

3.1.2. *Compressive strength*

The average compressive strengths of the specimens after different environmental actions are listed in Table 6. To analyze the effects of each factor and better explain the mechanism of the coupled actions, the compressive strength loss values were adopted, which can be defined as Eq. (1).

$$w_{cnu} = \frac{f_{cu} - f_{cun}}{f_{cu}} \times 100\% \quad (1)$$

where f_{cun} represents the strength of the concrete subjected to the durability test and f_{cu} represents the compressive strength of the control group.

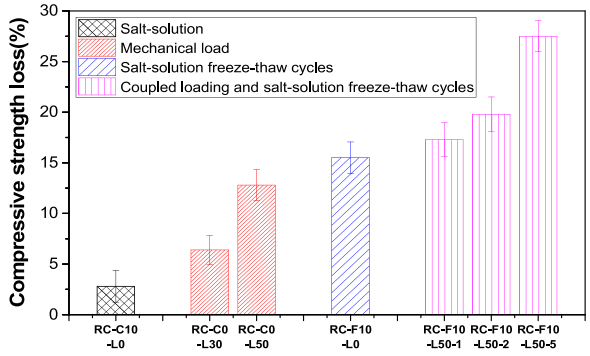

Fig. 9 – Compressive strength loss of recycled concrete subjected to various load and environmental actions.

The compressive strength loss values of each group are shown in Fig. 9. It can be seen that the compressive strength loss of the group under the coupled actions of mechanical load and salt-solution freeze-thaw cycles is the highest, which is followed by salt-solution freeze-thaw cycles and mechanical load. The compressive strength loss for the group subjected to salt-solution (RC-C10-L0) is the lowest, implying that the effect of salt corrosion on the durability of RC is negligible.

Test results also show that the compressive strength loss of the salt-solution group (RC-C10-L0) was 2.8%, while the compressive strength loss of the group under salt-solution freeze-thaw cycles (RC-F10-L0) was 15.5%. That is to say, the compressive strength loss is greatly increased owing to the combined freeze-thaw cycles. In addition, the compressive strength loss was increased from 12.8% to 27.5%, when the environmental action was changed from the mechanical load (RC-C0-L50) to the coupled actions of mechanical load and salt-solution freeze-thaw cycles (RC-F10-L50-5). It indicates that the compressive strength loss is greatly increased owing to the combined salt-solution freeze-thaw cycles. Apparently, the freeze-thaw cycles significantly affect the performance of RC.

Similarly, the compressive strength loss was increased from 15.5% to 27.5%, when the environmental action was changed from only salt-solution freeze-thaw cycles (RC-F10-L0) to the coupled actions of mechanical load and salt-solution freeze-thaw cycles (RC-F10-L50-5). It indicates the significant influence of the mechanical load on the performance of RC. On the other hand, the results of the mechanical load group show that the compressive strength loss was increased from 6.4% (RC-F0-L30) to 12.8% (RC-F0-L50), with the increase in the stress level. This demonstrates that the adverse effect of mechanical load on the RC performance is more obvious at high stress levels. Also, in the group under the coupled actions of mechanical load and salt-solution freeze-thaw cycles, the compressive strength loss increased from 17.3% (RC-F10-L50-1) to 27.5% (RC-F10-L50-5) with the increase in the alternative times of repetitive loading from 1 to 5.

3.2. *Effect of RA quality*

3.2.1. *Failure pattern*

During the compression test of the specimens after coupled actions (Fig. 10), cracks initially appeared at the inter-

(a) MRC-C50%-T4

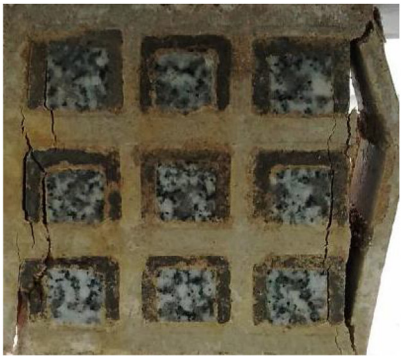

(b) MRC-C75%-T4

(c) MRC-C100%-T4

Fig. 10 – Damage patterns of modeled recycled concrete under compressive.

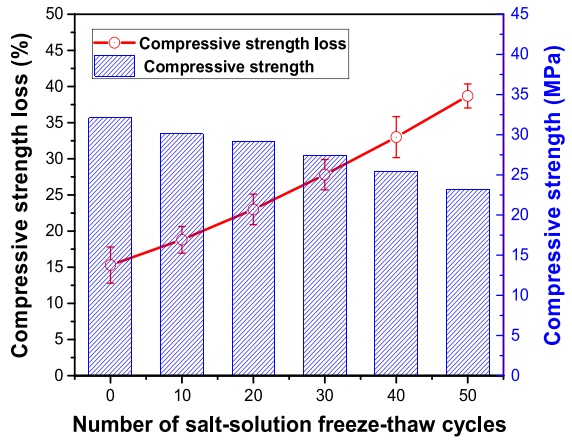

(a) Different initial damage of old mortar

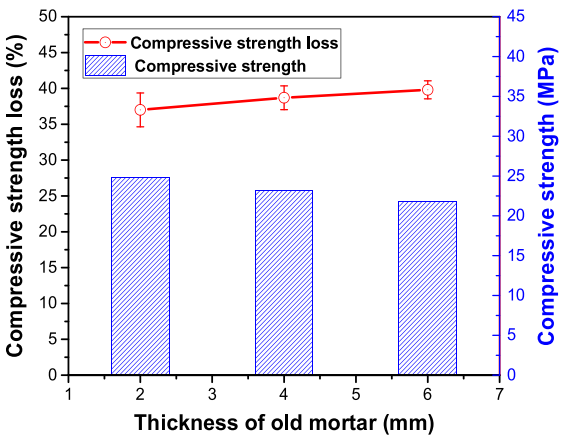

(b) Varying old mortar thickness

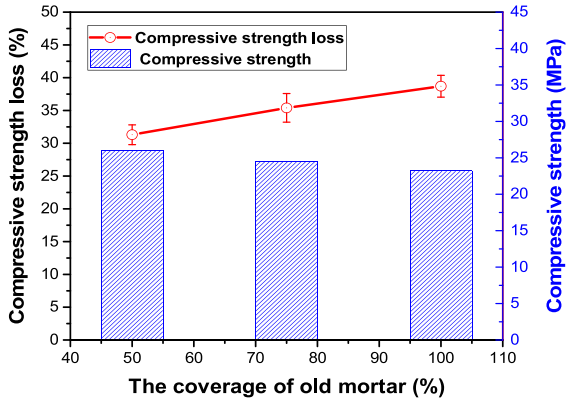

(c) Different coverage of old mortar

Fig. 11 – Compressive strength and compressive strength loss of MRC after coupled actions of mechanical load and salt-solution cycles.

face between the old mortar and natural aggregate. This means that the interface between the old mortar and natural aggregate is the weakest region in the RC. After that, cracks formed at the interface between the old mortar and the new mortar. Eventually, the specimens failed due to the connection of cracks and the peeling of mortar.

3.2.2. *Compressive strength*

The compressive strength and compressive strength loss of MRC after the coupled actions of mechanical load and salt-solution freeze-thaw cycles are shown in Fig. 11. According to Fig. 11(a), the compressive strength decreased, and the compressive strength loss of MRC increased, when the number of freeze-thaw cycles of MRA increased. For instance, the compressive strength of MRC decreased from 32.1 to 23.2 MPa, and the compressive strength loss of MRC increased from 15.3% to 38.7%, when the number of freeze-thaw cycles of MRA increased from 0 to 50. This implies that the durability of RC decreases with the increase in the initial damage of RA. From Fig. 11(b), it can be seen that the compressive strength decreased, and the compressive strength loss of MRC increased, as the thickness of the old mortar increased. For example, the compressive strength of MRC decreased from 24.8 to 21.8 MPa, and the compressive strength loss of MRC increased from 37% to 39.8%, when the thickness of the old mortar was increased from 2 mm to 6 mm. Therefore, the durability of RC slightly decreases with the increase in the thickness of the old mortar attached to RCA. From Fig. 11c, it shows that the compressive strength decreased, and the compressive strength loss of MRC increased, with the increase in the coverage of old mortar. Specifically, the compressive strength of MRC decreased from 26.0 to 23.2 MPa, and the compressive strength loss of MRC increased from 31.3% to 38.7%, when the coverage of the old mortar increased from 50% to 100%. Accordingly, the durability of RC decreases with the increase in the coverage of the adhered old mortar in RA. Moreover, it can be inferred from the results that the effect of the initial damage of old mortar on the durability of RC is more significant, in comparison with that of the thickness or coverage of the old mortar.

The initial damage of RA usually led to the stress concentration and crack initiation, as shown in Fig. 10, which resulted in performance degradation. Some studies have found that the

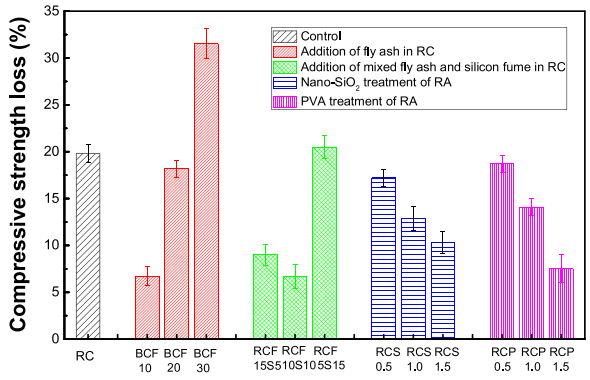

Fig. 12 – Compressive strength loss of modified RC subjected to coupled mechanical load and salt-solution freeze-thaw cycles.

adhered old cement mortar on RC is the weak point [42,52]. The poor performance of RC is associated with the cracks and fissures in the RA. These cracks and fissures make the RA weaker and more susceptible to permeation, diffusion, and fluids absorption [53]. The properties of RC are greatly affected by the property of the old mortar, and the RC with RA exhibiting excellent quality can perform excellently [54,55]. Liu et al. [4] found that the old mortar in RC has a great tendency to crack and fracture, while the fracture of the natural aggregate is rarely seen in NC.

On the other hand, the amount of adhered old cement mortar has an obvious effect on the RC durability, and the presence of high quantities of low-density old mortar in the RA would reduce the RC performance considerably. Xiao et al. [40] have concluded that the effective chloride diffusivity of RC increased with the increase in the content of the old adhered mortar. The mortar content affects the main properties of RA, such as absorption, density, Los Angeles abrasion, and sulfate content [56], because the adhered mortar is porous and presents numerous microcracks [57–59]. Therefore, removing the old mortar could enhance the performance of RC, and some methods for the removal of old mortar have been proposed [42].

3.3. *Modification treatments*

The compressive strength loss of the modified RC due to the coupled actions of mechanical load and salt-solution freeze-thaw cycles are shown in Fig. 12. For the RC with the addition of fly ash, when the cement was replaced by 10% and 20% fly ash, the compressive strength loss of the RC was lower than that of concrete without fly ash. However, when the fly ash content was increased to 30%, the compressive strength loss of RC was larger than that of the control RC without fly ash,

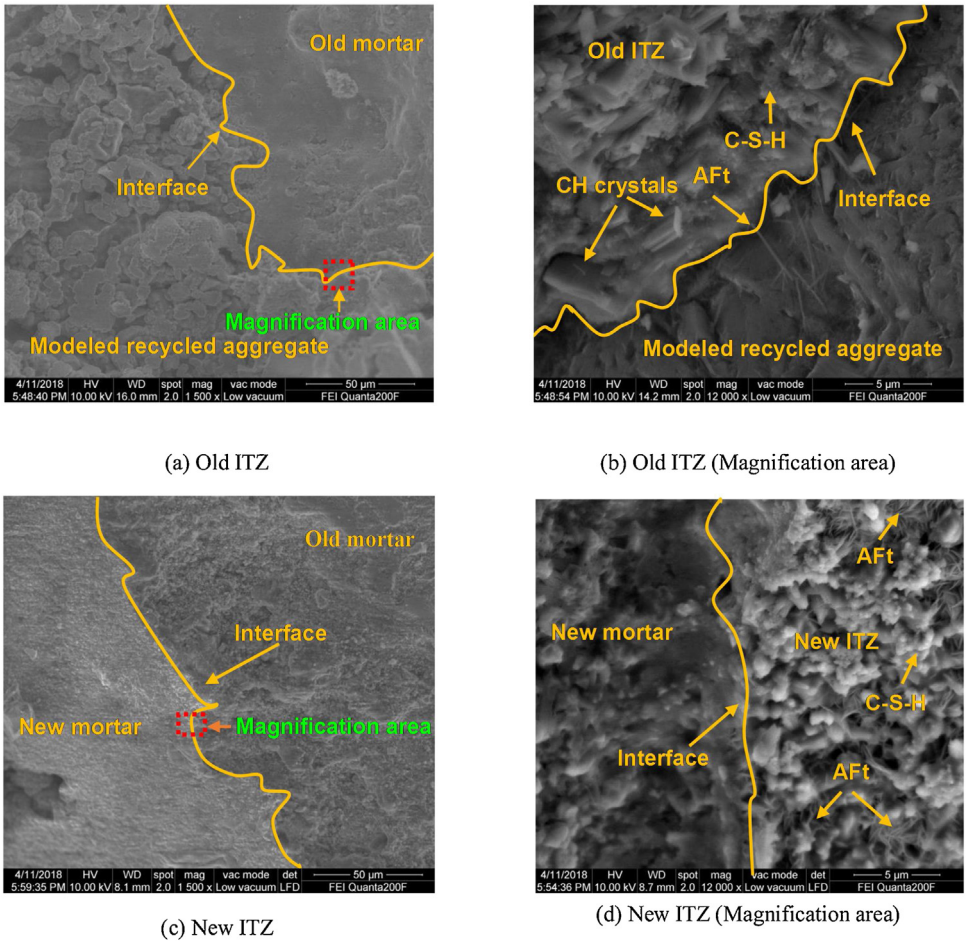

(a) Old ITZ

(b) Old ITZ (Magnification area)

(c) New ITZ

(d) New ITZ (Magnification area)

Fig. 13 – Microstructure of ITZs in MRC before coupled actions of loading and salt-solution freeze-thaw cycles.

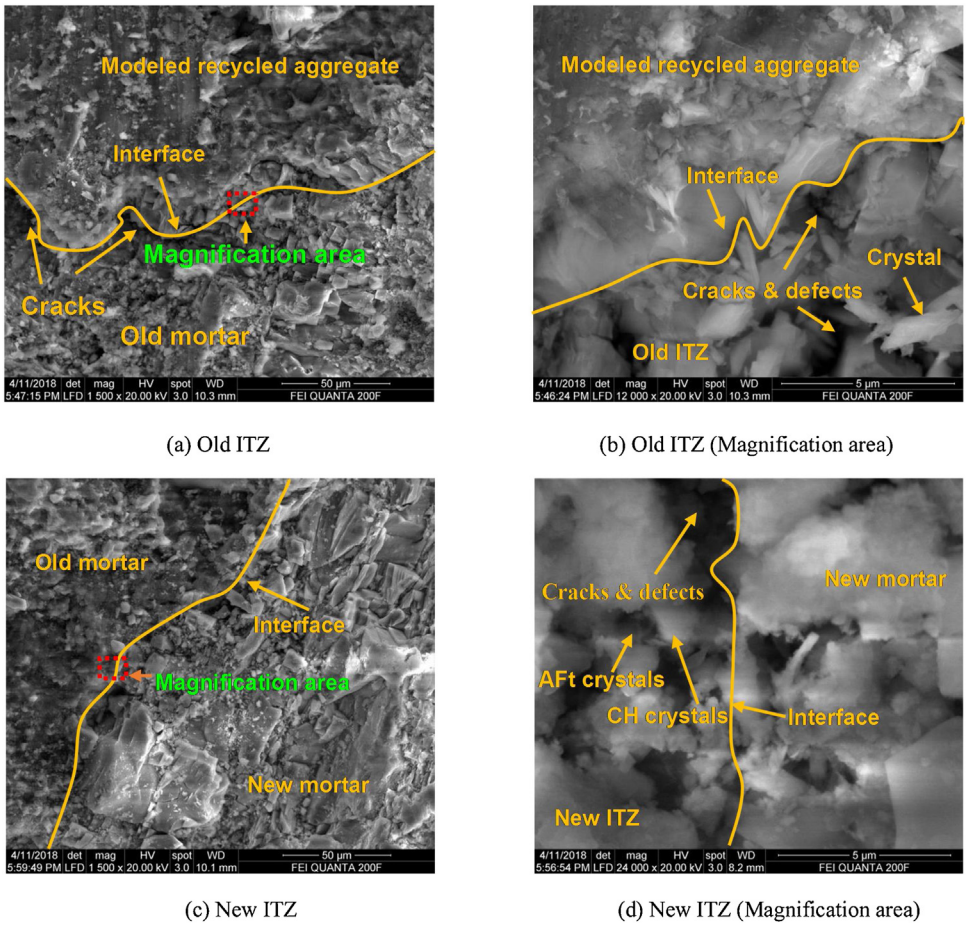

Fig. 14 – Microstructure of interfaces in MRC after coupled actions of mechanical loading and salt-solution freeze-thaw cycles.

demonstrating that the high fly ash content would reduce the performance of RC. Therefore, precautions should be taken to the fly ash content during the mixing proportion design of RC [60]. For instance, Arifi et al. [61] and Kou and Poon [62] recommended 25% as the optimum replacement ratio of cement by fly ash in RC.

As for the RC incorporated with the admixture of fly ash and silica fume, the compressive strength loss firstly decreased and then increased, with the increment of the silica fume content. Specifically, when the silica fume contents were 5% and 10%, the compressive strength loss of the RC was lower than that of the control RC without fly ash and the RC with 20% fly ash. It indicates that an improvement can be achieved by the inclusion of the admixture of fly ash and silica fume, and the effect is more obvious with the increase of the silica fume content. However, when the silica fume content was increased to 15%, the compressive strength loss of RC was larger than that of the RC with 20% fly ash and the RC without fly ash. Therefore, proper mixing of fly ash and silica fume can increase the durability of RC. Silica fume is known to improve the strength and durability of concrete, due to the effects of pores filling, pozzolanic reaction, and interfacial zone enhancement [63]. However, excessive silica fume can have adverse effects on the workability and dry shrinkage properties of concrete [63].

Additionally, Fig. 12 shows that when the concentration of the nano-SiO_2 solution and PVA emulsion was 0.5%, the compressive strength loss of the concrete with modified RA was close to that of the control RC. However, with the increase in the concentrations of PVA emulsion and nano-SiO_2 solution, the compressive strength loss decreased continuously. For instance, when the content was 1.5%, the compressive strength loss was reduced from 19.8% to 10.3% and 7.5%, respectively, after the treatment by PVA emulsion and nano-SiO_2 solution. It has been reported that impregnation treatments of RA have many benefits: the voids and cracks on the surface of RA can be filled, and the interface structure can be enhanced [34]. Even though, it should be noted that there are some limitations of RA impregnation treatments, especially in terms of cost and practical handling issues, which highlights the necessity of relevant studies in the future [34,46,48].

3.4. *Microstructure characterization*

The microstructures of ITZs in MRC characterized by SEM are shown in Figs. 13 and 14. Before the coupled actions of mechanical load and salt-solution freeze-thaw cycles, a large number of worm-like calcium silicate hydrate (C-S-H) gels, mixed with plate-shaped calcium hydroxide (CH) crystals and

a small amount of rod-like Ettringite (AFt) crystals, could be observed in the old ITZ. Additionally, obvious cracks can be identified in the old ITZ, which led to the poor connection between the aggregate and old cement mortar. While in the new ITZ, flocs of C-S-H gels are tightly bonded, and the rod-like crystals are interspersed between the gels. It would result in the increased stability of the microstructure and high bond strength.

After the coupled actions of mechanical load and salt-solution freeze-thaw cycles, cracks could be identified in both the old and new ITZs. By comparing Figs. 13 and 14, it could also be found that the flocs of C-S-H gel were reduced considerably. In addition, short rod-like AFt crystals and six square plate-like CH crystals, which were originally encapsulated by C-S-H gel, were gradually formed and accumulated in the pores or cracks. It finally makes the ITZ micromorphology rough and messy.

4. Conclusions

The effects of environmental actions, recycled aggregate quality, and modification treatments on the durability of recycled concrete were investigated in this study. The main conclusions are drawn up as follows:

(1) The deterioration of RC under the coupled actions of mechanical load and salt-solution freeze-thaw cycles was the most severe, followed by the salt-solution freeze-thaw cycles, mechanical load, and salt-solution. The durability of RC after the coupled actions of mechanical load and salt-solution freeze-thaw cycles deteriorated more significantly, as the alternative times of repetitive loading increased.
(2) Cracks first appeared at the interfaces between the old mortar and MRA, which was the weakest zone in the RC. With the increase in the old mortar thickness, old mortar coverage, or the initial damage, the durability of RC was declined. Also, the effect of the initial damage of the old mortar was more significant than that of the thickness or coverage of old mortar.
(3) Treating the RA with 1.5% nano-SiO_2 and 1.5% PVA emulsion, and replacing the cement with 10% fly ash could greatly improve the resistance of the RC to the coupled actions of mechanical load and salt-solution freeze-thaw cycles. Specifically, the compressive strength loss of the concrete is reduced from 19.8% to 9%, 10.3%, and 7.5% after the above treatment methods, respectively.
(4) After subjected to the coupled actions of mechanical load and salt-solution freeze-thaw cycles, cracks and large particles of recycled concrete can be identified at both the old and new ITZs, manifesting the rough and messy micromorphology.

Conflict of interest

The authors declare no conflicts of interest.

Acknowledgments

This research was supported by the National Natural Science Foundation of China (51968046; 51668045), Australian Research Council (DE150101751; DP200100057; IH150100006; IH200100010) and University of Technology Sydney Research Academic Program at Tech Lab (UTS RAPT).

REFERENCES

[1] Xiao JZ, Li WG, Fan YH, Huang X. An overview of study on recycled aggregate concrete in China (1996–2011). Constr Build Mater 2012;31(6):364–83.
[2] Saha AK, Majhi S, Sarker PK, Mukherjee A, Siddika A, Aslani F, et al. Non-destructive prediction of strength of concrete made by lightweight recycled aggregates and nickel slag. J Build Eng 2021;33:101614.
[3] Ulsen C, Tseng E, Angulo SC, et al. Concrete aggregates properties crushed by jaw and impact secondary crushing. J Mater Res Technol 2019;8:494–502.
[4] Lei B, Li W, Liu H, Tang Z, Tam VWY. Synergistic effects of polypropylene and glass fiber on mechanical properties and durability of recycled aggregate concrete. Int J Concr Struct Mater 2020;14:37.
[5] Tang Z, Li W, Tam VWY, Yan L. Mechanical performance of CFRP-confined sustainable geopolymeric recycled concrete under axial compression. Eng Struct 2020;224:111246.
[6] Rahal K. Mechanical properties of concrete with recycled coarse aggregate. Build Environ 2007;42(1):407–15.
[7] Xiao JZ, Lei B, Zhang CZ. On carbonation behavior of recycled aggregate concrete. Sci China Tech Sci 2012;55(9):2609–16.
[8] Zhang KJ, Xiao JZ. Prediction model of carbonation depth for recycled aggregate concrete. Cem Concr Compos 2018;88:86–99.
[9] Bravo M, de Brito J, Pontes J, Evangelista L. Durability performance of concrete with recycled aggregates from construction and demolition waste plants. Constr Build Mater 2015;77:357–69.
[10] Dimitriou G, Savva P, Petrou M. Enhancing mechanical and durability properties of recycled aggregate concrete. Constr Build Mater 2018;158:228–35.
[11] Vázquez E, Marilda BB, Diego A, Cristián J, Susanna V. Improvement of the durability of concrete with recycled aggregates in chloride exposed environment. Constr Build Mater 2014;67:61–7.
[12] Iii WVS. Stochastic service-life modeling of chloride-induced corrosion in recycled-aggregate concrete. Cem Concr Compos 2015;55:103–11.
[13] Bulatović V, Melešev M, Radeka M, Radonjanin V, Lukic I. Evaluation of sulfate resistance of concrete with recycled and natural aggregates. Constr Build Mater 2017;152:614–31.
[14] Qi B, Gao J, Chen F, Shen D. Evaluation of the damage process of recycled aggregate concrete under sulfate attack and wetting-drying cycles. Constr Build Mater 2017;138:254–62.
[15] Zega CJ, Coelho Dos Santos GS, Villagrán-Zaccardi YA, Di Maio AA. Performance of recycled concretes exposed to sulphate soil for 10 years. Constr Build Mater 2016;102:714–21.
[16] Salem RM, Burdette EG, Jackon NM. Resistance to freezing and thawing of recycled aggregate concrete. ACI Mater J 2000;100(3):216–21.
[17] Li SG, Chen GX, Ji GJ, Lu YH. Quantitative damage evaluation of concrete suffered freezing-thawing by DIP technique. Constr Build Mater 2014;69:177–85.

[18] Richardson A, Coventry K, Bacon J. Freeze/thaw durability of concrete with recycled demolition aggregate compared to virgin aggregate concrete. J Clean Prod 2011;19:272–7.
[19] Huda SB, Shahria Alam M, 2009 Mechanical and freeze-thaw durability properties of recycled aggregate concrete made with recycled coarse aggregate. J Mater Civil Eng 2015;27(10):04015003.
[20] Abbas A, Fathifazl G, Isgor OB, Razaqpur AG, Fournier B, Foo S, 2009 Durability of recycled aggregate concrete designed with equivalent mortar volume method. Cem Concr Compos 2009;31:555–63.
[21] Wang WJ, Wu J, Wang Z, Wu GZ, Yue AY. Chloride diffusion coefficient of recycled aggregate concrete under compressive loading. Mater Struct 2016;49:4729–96.
[22] Kim D, Shimura K, Horiguchi T. Effect of tensile loading on chloride penetration of concrete mixed with granulated blast furnace slag. J Adv Concr Technol 2010;8:27–34.
[23] Rahman MK, Al-Kutti WA, Shazali MA, Baluch MH. Simulation of chloride migration in compression-induced damage in concrete. J Mater Civil Eng 2012;24:789–96.
[24] Qiao Y, Sun W, Jiang J. Damage process of concrete subjected to coupling fatigue load and freeze/thaw cycles. Constr Build Mater 2015;93:806–11.
[25] Kosior-Kazberuk M, Berkowski P. Surface scaling resistance of concrete subjected to freeze-thaw cycles and sustained load. Procedia Eng 2017;172:513–20.
[26] Sun W, Zhang YM, Yan HD, Mu R. Damage and damage resistance of high strength concrete under the action of load and freeze-thaw cycles. Cem Concr Res 1999;29(9):1519–23.
[27] Mu R, Miao C, Luo X, Sun W. Interaction between loading, freeze-thaw cycles, and chloride salt attack of concrete with and without steel fiber reinforcement. Cem Concr Res 2002;32:1061–6.
[28] Lei B, Li WG, Tam VWY, Sun ZH. Investigation on properties of recycled aggregate concrete under coupling loading and freeze-thaw cycles in salt-solution. Constr Build Mater 2018;163:840–9.
[29] Li WG, Luo ZY, Long C, Wu CQ, Duan WH, Shah SP. Effects of nanoparticle on the dynamic behaviors of recycled aggregate concrete under impact loading. Mater Design 2016;112:58–66.
[30] Poon CS, Shui ZH, Lam L. Effect of microstructure of ITZ on compressive strength of concrete. Constr Build Mater 2004;18:461–8.
[31] Li W, Luo Z, Sun Z, Hu Y, Duan WH. Numerical modelling of plastic–damage response and crack propagation in RAC under uniaxial loading. Mag Concr Res 2018;70(9):459–72.
[32] Marí A, Etxeberria M, Vázquez E. Microstructure analysis of hardened recycled aggregate concrete. Mag Concr Res 2006;58(10):683–90.
[33] Nagataki S, Gokce A, Saeki T, Hisada M. Assessment of recycling process induced damage sensitivity of recycled concrete aggregates. Cem Concr Res 2004;34(6): 965–71.
[34] Tam VWY, Gao XF, Tam CM. Microstructural analysis of recycled aggregate concrete produced from two-stage mixing approach. Cem Concr Res 2005;35(6):1195–203.
[35] Yildirim ST, Meyer C, Herfellner S. Effects of internal curing on the strength, drying shrinkage and freeze-thaw resistance of concrete containing recycled concrete aggregates. Constr Build Mater 2015;91:288–96.
[36] Barra de Oliveira M, Vazquez E. The influence of retained moisture in aggregates from recycling on the properties of new hardened concrete. Waste Manag 1996;16:113–7.
[37] Chen ZY, Wang JG. Bond between marble and cement paste. Cem Concr Res 1987;17(4):544–52.
[38] Zimbelmann R. A contribution to the problem of cement-aggregate bond. Cem Concr Res 1985;15(5):801–8.
[39] Duan ZH, Poon CS. Properties of recycled aggregate concrete made with recycled aggregates with different amounts of old adhered mortars. Mater Design 2014;58(6):19–29.
[40] Xiao JZ, Ying JW, Shen LM. FEM simulation of chloride diffusion in modeled recycled aggregate concrete. Constr Build Mater 2012;29:12–23.
[41] Xiao JZ, Li W, Corr DJ, Shah SP. Effects of interfacial transition zones on the stress-strain behavior of modelled recycled aggregate concrete. Cem Concr Res 2013;52:82–9.
[42] Shi CJ, Li YK, Zhang JK, Li WG, Chong LL, Xie ZB. Performance enhancement of recycled concrete aggregate–a review. J Clean Prod 2016;112:466–72.
[43] Lei B, Li W, Li Z, Wang G, Sun Z. Effect of cyclic loading deterioration on concrete durability: water absorption, freeze-thaw, and carbonation. J Mater Civil Eng 2018;30(9):04018220.
[44] Mukharjee BB, Barai SV. Influence of nano-silica on the properties of recycled aggregate concrete. Constr Build Mater 2014;55:29–37.
[45] Luo ZY, Li WG, Tam VWY, Xiao JZ, Shah SP. Current progress on nanotechnology application in recycled aggregate concrete. J Sustainable Cem Based Mater 2018;8(2):79–96.
[46] Zhang HR, Zhao YX, Tao M, Surendra PS. Surface treatment on recycled coarse aggregates with nanomaterials. J Mater Civil Eng 2016;28(2):04015094.
[47] Kou SC, Poon CS. Properties of concrete prepared with PVA-impregnated recycled concrete aggregates. Cem Concr Compos 2010;32(8):649–54.
[48] Mansur A, Santos D, Mansur H. A microstructural approach to adherence mechanism of poly (vinyl alcohol) modified cement systems to ceramic tiles. Cem Concr Res 2007;37(2):270–82.
[49] GB/T50081-5. In: Test Method for Mechanical Properties of Ordinary Concrete. China: China Architecture and Building Press; 2002.
[50] GB/T50082-5. In: Standard for Test Method of Long-Term Performance and Durability of Ordinary Concrete. China: China Architecture and Building Press; 2009.
[51] Al-Amoudi OSB. Attack on plain and blended cements exposed to aggressive sulfate environments. Cem Concr Compos 2002;24(3-4):305–16.
[52] Etxeberria M, Vazquez E, Mari A. Microstructure analysis of hardened recycled aggregate concrete. Mag Concr Res 2006;58(10):683–90.
[53] Olorunsogo FT, Padayachee N. Performance of recycled aggregate concrete monitored by durability indexes. Cem Concr Res 2002;32:179–85.
[54] Padmini AK. Influence of parent concrete on the properties of recycled aggregate concrete. Constr Build Mater 2009;23:829–36.
[55] Kou SC, Poon CS. Effect of the quality of parent concrete on the properties of high performance recycled aggregate concrete. Constr Build Mater 2015;77:501–8.
[56] de Juan MS, Gutiérrez PA. Study on the influence of attached mortar content on the properties of recycled concrete aggregate. Constr Build Mater 2009;23(2):872–7.
[57] Rao A, Jha KN, Misra S. Use of aggregates from recycled construction and demolition waste in concrete. Resour Conserv Recycl 2007;50(1):71–81.
[58] Abbas A, Fathifazl G, Fournier B, Isgor OB, Zavadil R, Razaqpur AG, et al. Quantification of the residual mortar content in recycled concrete aggregates by image analysis. Mater Charact 2009;60(7):716–28.
[59] Tang Z, Li WG, Tam VWY, Yan LB. Mechanical behaviors of CFRP-confined sustainable geopolymeric recycled aggregate concrete under both static and cyclic compressions. Compos Struct 2020;252:112750, http://dx.doi.org/10.1016/j.compstruct.2020.112750.

[60] Bilodeau A, Sivasundaram V, Painter KE, Malhotra VM. Durability of concrete incorporating high volume of fly-ash from source in the US. ACI Mater J 1994;91(1):3–12.
[61] Arifi E, Zacoeb A, Shigeishi M. Effect of fly ash on the strength of concrete made from recycled aggregate by pulsed power. Int J Geomate 2014;7(1):1009–16.
[62] Kou SC, Poon CS. Long-term mechanical and durability properties of recycled aggregate concrete prepared with the incorporation of fly ash. Cem Concr Compos 2013;37:12–9.
[63] Zhang P, Li QF. Effect of silica fume on durability of concrete composites containing fly ash. Sci Eng Compos Mater 2013;20(1):57–65.